JP0050135

JAERI-Research
99-072

VACUUM DISCHARGE AS A POSSIBLE SOURCE OF GAMMA-RAY BURSTS

December 1999

Guangjun MAO*, Satoshi CHIBA, Walter GREINER* and
Kazuhiro OYAMATSU*

日本原子力研究所
Japan Atomic Energy Research Institute

本レポートは、日本原子力研究所が不定期に公刊している研究報告書です。
入手の問合わせは、日本原子力研究所研究情報部研究情報課（〒319-1195　茨城県那珂郡東海村）あて、お申し越し下さい。なお、このほかに財団法人原子力弘済会資料センター（〒319-1195　茨城県那珂郡東海村日本原子力研究所内）で複写による実費領布を行っております。

This report is issued irregularly.
Inquiries about availability of the reports should be addressed to Research Information Division, Department of Intellectual Resources, Japan Atomic Energy Research Institute, Tokai-mura, Naka-gun, Ibaraki-ken 319-1195, Japan.

編集兼発行　日本原子力研究所

JAERI－Research 99－072

Vacuum Discharge as a Possible Source of Gamma-ray Bursts

Guangjun MAO*1, Satoshi CHIBA, Walter GREINER*2 and Kazuhiro OYAMATSU*3

Advanced Science Research Center
(Tokai-Site)
Japan Atomic Energy Research Institute
Tokai-mura, Naka-gun , Ibaraki-ken

(Received December 1, 1999)

We propose that spontaneous particle–anti-particle pair creations from the discharged vacuum caused by the strong interactions in dense matter are major sources of γ-ray bursts. Two neutron star collisions or black hole-neutron star mergers at cosmological distance could produce a compact object with its density exceeding the critical density for pair creations. The emitted anti-particles annihilate with corresponding particles at the ambient medium. This releases a large amount of energy. We discuss the spontaneous $p\bar{p}$ pair creations within two neutron star collision and estimate the exploded energy from $p\bar{p}$ annihilation processes. The total energy could be around $10^{51} - 10^{53}$ erg depending on the impact parameter of colliding neutron stars. This value fits well into the range of the initial energy of the most energetic γ-ray bursts. We suggest to measure the anti-proton spectra from the identical sources of γ-ray bursts to test the scenario.

Keywords : Gamma-ray Bursts, Particle–anti-particle Pair Creations, Vacuum Discharge in Dense Matter, Strong Interactions, Neutron Stars

*1 STA Fellow
*2 J.W. Goethe-Universität, Postfach 11 19 32, D-60054 Frankfurt am Main, Germany
*3 Aichi Shukutoku University, 9 Katahira, Nagakute, Aichi 480-1197, Japan

ガンマ線バーストの起源としての真空からの自発的粒子・反粒子生成の可能性

日本原子力研究所先端基礎研究センター
茅　廣軍[*1]・千葉　敏・W. Greiner[*2]・親松　和浩[*3]

(1999 年 12 月 1 日受理)

高密度物質中での強い相互作用によって起こる真空 (Dirac 海) からの自発的な粒子・反粒子生成によってガンマ線バーストのエネルギーが説明できることを示す。我々のモデルでは、生成された反粒子が周囲に存在する物質中で対応する同種粒子と対消滅し非常に大きなエネルギーを放出し、それがガンマ線バーストのエネルギー源となる。このような粒子・反粒子対生成を起こすのに必要な臨界密度以上の高密度物質を作る候補としては、二つの中性子星の衝突、またはブラックホールと中性子星の合体が考えられる。そこで、二つの中性子星の衝突の場合に起こる陽子・反陽子生成と引き続き起こる対消滅によるエネルギー放出量を推定し、約 10^{51}から 10^{53} erg (衝突係数によって異なる) という値を得た。この値は、最もエネルギーの大きいガンマ線バーストの初期エネルギーとして観測より推定されている値と一致する。本研究において我々が提案したシナリオを検証するために、ガンマ線バースト源からの反陽子スペクトルを測定することを提案する。

日本原子力研究所（東海駐在): 〒 319-1195 茨城県那珂郡東海村白方白根 2-4
*1 STA フェロー
*2 フランクフルト大学 : Postfach 11 19 32, D-60054 Frankfurt am Main, Germany
*3 愛知淑徳大学 : 〒 480-1197 愛知県長久手町長湫片平 9

Contents

目　　次

This is a blank page.

I. INTRODUCTION

Gamma-ray bursts (GRBs) were discovered accidentally in the late 1960s by the Vela satellites. It was announced in 1973 [1]. Since then, they have been one of the greatest mysteries in high-energy astrophysics for almost 30 years. The situation was improved dramatically in 1997, when the BeppoSAX satellite discovered X-ray afterglow [2], this enabled accurate position determination and the discovery of optical [3] and radio [4] afterglows and host galaxies. The distance scale to GRBs was finally unambiguously determined: their sources are at cosmological distances [5]. In spite of all these recent progresses, we still do not know what produces GRBs! The nature of the underlying physical mechanism that powers these sources remains unclear. The optical identification and measurement of redshifts for GRBs allow us to determine their distances and the amount of energy that would be radiated in an isotropic explosion. In recent three observations (GRB971214 [6], 980703 [7] and 990123 [8]), the total isotropic energy radiated is estimated to be in excess of 10^{53} erg. For GRB990123, the inferred isotropic energy release is up to 3.4×10^{54} erg, or 1.9 $M_\odot$ (where $M_\odot$ is the solar mass), which is larger than the rest mass of most neutron stars. It has been suggested that the explosion of GRB990123 is not isotropic, which reduces the energy released in γ-rays alone to be 6×10^{52} erg [8] due to finite beaming angle. However, if one adopts the picture of the fireball internal shocks model [9] that random internal collisions among shells produce the highly variable γ-ray burst emissions, the required initial energy will be raised by a factor of about 100 since it is argued that only 1% of the energy of the initial explosion can be converted to the observed radiation [10]. Therefore, it appears that the total exploded energy for the most energetic bursts is close to or possibly greater than 10^{54} erg. It seems to be difficult to imagine a source that could provide so much energy. The first and foremost open question concerning GRBs is what are the inner engines that power GRBs [9] ?

On the other hand, the GRB spectrum is nonthermal. In most cases there is a strong power law high-energy tail extending to a few GeV. A particular high-energy tail up to 18 GeV has been reported in GRB940217 [11]. This nonthermal spectrum provides an important clue to the nature of GRBs.

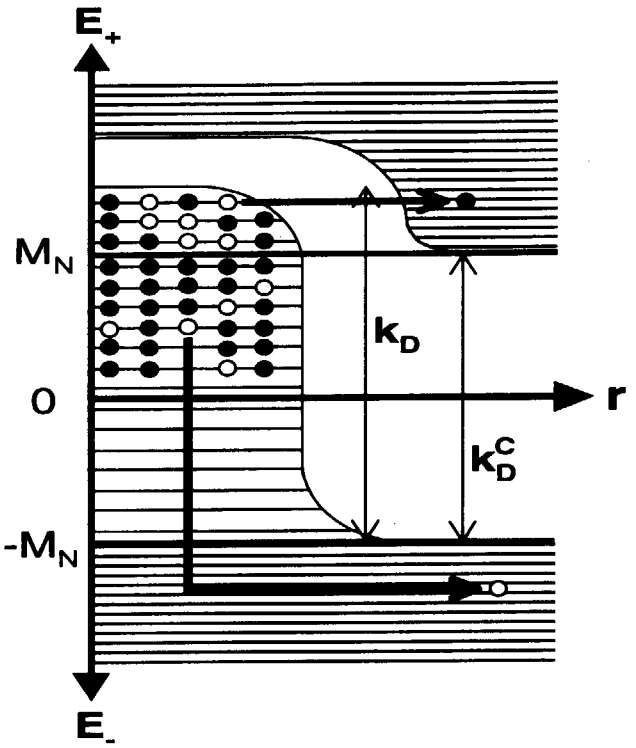

FIG. 1. Schematic view of $N\bar{N}$ pair creation from the Dirac sea due to strong fields in dense matter.

Various GRB models have been suggested in the literature, e.g., Refs. [9,12,15–18]. Among them, the neutron star merger seems to be the most promising candidate. Three-dimensional hydrodynamical simulations of the coalescence of binary neutron stars (NS-NS) [13–15,19], direct collision of two neutron stars [20–22] as well as black hole-neutron star (BH-NS) merger [23] have been performed by some authors. The largest energy deposition of $\sim 10^{51}$ erg by $\nu\bar{\nu}$ annihilation was obtained in the black hole-neutron star merger. This may account for certain low-energy GRBs on the one hand, is, on the other hand, still far away from the energetic ones mentioned above. However, it should be pointed out that in those macroscopic simulations (and almost all GRB fireball models) the effects of strong interactions, e.g., the modification of hadron properties in dense matter, many body effects, vacuum correlations et al., have been largely neglected except a nuclear equation of state is applied.

In this work we propose an alternative scenario for the source of the most energetic γ-ray bursts. It is well known that the density is fairly high at the center of neutron star. The central density can be several times nuclear saturation density [24]. Furthermore, superdense matter could be formed at NS-NS/BH-NS merger and direct NS-NS collision. Three-dimensional hydrodynamical simulations showed that when two neutron stars collide, the maximum density of the compressed core can be 1.4 (off-center collision, the impact parameter $b = R$, i.e., one neutron star radius) to 1.9 (head-on collision) times of the central density of a single neutron star [22]. At such high density, not only the properties of baryons will be modified drastically according to the investigation of relativistic mean-field theory (RMF) and relativistic Hartree approach (RHA) [25], but also the vacuum, i.e., the lower Dirac sea, might be distorted substantially [26] since the meson fields, which describe the strong interactions between baryons, are very large. At certain densities, when the negative energy of the nucleons in the Dirac sea is larger than the nucleon free mass, the nucleon–anti-nucleon pairs can be created spontaneously from the vacuum [27,28]. A schematic picture for this phenomena is depicted in Fig. 1. The situation is quite similar to the electron-positron pair creations in QED with strong electromagnetic fields. The produced anti-nucleons will then annihilate with the nucleons at the ambient medium through the $N\bar{N} \rightarrow \gamma\gamma$ reaction. This yields a large amount of energy and photons. The sequent process, $\gamma\gamma \leftrightarrow e^+e^-$, inevitably leads to the creation of a fireball. The dynamical expansion of the fireball will radiate the observed γ-rays through the nonthermal processes in shocks [9]. In the following sections, we shall estimate whether enough energy is available within this scenario to satisfy the requirement of a source of energetic GRBs. The report is organized as follows: In Sect. II we introduce our theoretical framework. In Sect. III we present numerical results for the properties of neutron star matter and neutron star structure. In Sect. IV we discuss two neutron star collisions and estimate the released energy. Finally, a summary and outlook is given in sect. V.

II. THEORY

We start from the Lagrangian density for nucleons interacting through the exchange of mesons

$$\begin{aligned}\mathcal{L} = &\bar{\psi}[i\gamma_\mu\partial^\mu - M_N]\psi + \frac{1}{2}\partial_\mu\sigma\partial^\mu\sigma - \frac{1}{2}m_\sigma^2\sigma^2 - \frac{1}{4}\omega_{\mu\nu}\omega^{\mu\nu} \\ &+\frac{1}{2}m_\omega^2\omega_\mu\omega^\mu - \frac{1}{4}\mathbf{R}_{\mu\nu}\mathbf{R}^{\mu\nu} + \frac{1}{2}m_\rho^2\mathbf{R}_\mu\cdot\mathbf{R}^\mu \\ &+\mathrm{g}_\sigma\bar{\psi}\psi\sigma - \mathrm{g}_\omega\bar{\psi}\gamma_\mu\psi\omega^\mu - \frac{1}{2}\mathrm{g}_\rho\bar{\psi}\gamma_\mu\boldsymbol{\tau}\cdot\psi\mathbf{R}^\mu, \end{aligned} \tag{1}$$

where ψ is the Dirac spinor of the nucleon; σ, ω_μ and $\mathbf{R}_\mu$ represent the scalar meson, vector meson and isovector-vector meson field, respectively. Here the field tensors for the omega and rho are given in terms of their potentials by

$$\omega_{\mu\nu} = \partial_\mu\omega_\nu - \partial_\nu\omega_\mu, \tag{2}$$

$$\mathbf{R}_{\mu\nu} = \partial_\mu\mathbf{R}_\nu - \partial_\nu\mathbf{R}_\mu. \tag{3}$$

Based on this Lagrangian, we have developed a relativistic Hartree approach including vacuum contributions which describes the properties of nucleons and anti-nucleons in nuclear matter and finite nuclei quite successfully [28]. The model can be further applied to the neutron, proton and electron (n-p-e) system under the beta equilibrium and the charge neutrality conditions which is in particular important for the neutron star. The Dirac equation for the nucleons can be written as

$$\left[i\gamma_\mu\partial^\mu - \mathrm{g}_\omega\gamma_\mu\omega^\mu - \frac{1}{2}\mathrm{g}_\rho\gamma_\mu\tau_0 R_0^\mu - M_N + \mathrm{g}_\sigma\sigma\right]\psi = 0. \tag{4}$$

In static neutron star matter, the above equation can be solved immediately to yield the positive energy of the nucleons in the Fermi sea E_+ and the negative energy of the nucleons in the Dirac sea E_- which read as

$$E_+ = \left\{\left[k^2 + (M_N - \mathrm{g}_\sigma\sigma)^2\right]^{1/2} + \mathrm{g}_\omega\omega_0 + \frac{1}{2}\mathrm{g}_\rho\tau_0 R_{0,0}\right\}, \tag{5}$$

$$E_- = -\left\{\left[k^2 + (M_N - \mathrm{g}_\sigma\sigma)^2\right]^{1/2} - \mathrm{g}_\omega\omega_0 + \frac{1}{2}\mathrm{g}_\rho\tau_0 R_{0,0}\right\}. \tag{6}$$

The energy of anti-nucleons $\bar{E}_+$ is just the minus sign of E_-, i.e., $\bar{E}_+ = -E_-$ [28]. Here σ, ω_0 and $R_{0,0}$ are the mean values of the scalar field, the time-like component of the vector field, and the time-like isospin 3-component of the vector-isovector field in neutron star matter, respectively. They are obtained by solving the non-linear equations of the meson felds

$$m_\sigma^2 \sigma = \mathrm{g}_\sigma \left(\rho_S^{val} + \rho_S^{sea} \right), \tag{7}$$

$$m_\omega^2 \omega_0 = \mathrm{g}_\omega \rho_0^{val}, \tag{8}$$

$$m_\rho^2 R_{0,0} = \frac{1}{2} \mathrm{g}_\rho \rho_{0,0}^{val}. \tag{9}$$

Here ρ_S^{val}, ρ_0^{val} and $\rho_{0,0}^{val}$ are the scalar density, the time-like component of the vector density and the time-like isospin 3-component of the vector-isovector density contributed from the valence nucleons, that is, from the Fermi sea; ρ_S^{sea} is the scalar density contributed from the Dirac sea, respectively. They can be written as

$$\rho_S^{val} = \sum_{\alpha=p,n} \frac{m^*}{2\pi^2} \left[k_F^\alpha \mu_\alpha^* - m^{*2} \ln \frac{k_F^\alpha + \mu_\alpha^*}{m^*} \right], \tag{10}$$

$$\rho_S^{sea} = -\frac{1}{\mathrm{g}_\sigma} \frac{\partial}{\partial \sigma} \left[V_F^{(1)}(\sigma) \right], \tag{11}$$

$$\rho_0^{val} = \rho_0^p + \rho_0^n, \tag{12}$$

$$\rho_{0,0}^{val} = \rho_0^p - \rho_0^n, \tag{13}$$

where

$$\rho_0^p = \frac{(k_F^p)^3}{3\pi^2}, \tag{14}$$

$$\rho_0^n = \frac{(k_F^n)^3}{3\pi^2}, \tag{15}$$

$$m^* = M_N - \mathrm{g}_\sigma \sigma, \tag{16}$$

$$\mu_\alpha^* = \left[(k_F^\alpha)^2 + m^{*2} \right]^{1/2}. \tag{17}$$

The $V_F^{(1)}(\sigma)$ is obtained through evaluating the one-nucleon loop, which turns out to be [25,29]

$$V_F^{(1)}(\sigma) = -\frac{1}{4\pi^2} \left[(M_N - \mathrm{g}_\sigma \sigma)^4 \ln \left(1 - \frac{\mathrm{g}_\sigma \sigma}{M_N} \right) + M_N^3 \mathrm{g}_\sigma \sigma - \frac{7}{2} M_N^2 \mathrm{g}_\sigma^2 \sigma^2 + \frac{13}{3} M_N \mathrm{g}_\sigma^3 \sigma^3 - \frac{25}{12} \mathrm{g}_\sigma^4 \sigma^4 \right]. \tag{18}$$

The chemical potentials of nucleons and electrons are defined as

$$\mu_p = \mu_p^* + g_\omega \omega_0 + \frac{1}{2} g_\rho R_{0,0}, \tag{19}$$

$$\mu_n = \mu_n^* + g_\omega \omega_0 - \frac{1}{2} g_\rho R_{0,0}, \tag{20}$$

$$\mu_e = \left[(k_F^e)^2 + m_e^2 \right]^{1/2}. \tag{21}$$

In above equations, k_F^p, k_F^n and k_F^e are the Fermi momenta of proton, neutron and electron, respectively. The total baryon number density $\rho = \rho_0^p + \rho_0^n$; the electron density $\rho^e = (k_F^e)^3/3\pi^2$. The non-linear meson equations of (7) $\sim$ (9) are solved self-consistently in a numerical procedure with respect to the constraints of the charge neutrality

$$\rho_0^p = \rho^e \tag{22}$$

and the β-equilibrium

$$\mu_n = \mu_p + \mu_e. \tag{23}$$

The total energy density and pressure of the system can then be calculated by means of the following formula

$$\begin{aligned}
\epsilon = & \frac{1}{2} m_\sigma^2 \sigma^2 + \frac{1}{2} m_\omega^2 \omega_0^2 + \frac{1}{2} m_\rho^2 R_{0,0}^2 \\
& + \sum_{\alpha=p,n} \frac{1}{4\pi^2} \left[k_F^\alpha \mu_\alpha^{*3} - \frac{m^{*2}}{2} k_F^\alpha \mu_\alpha^* - \frac{m^{*4}}{2} \ln \left(\frac{k_F^\alpha + \mu_\alpha^*}{m^*} \right) \right] \\
& + \frac{1}{4\pi^2} \left[k_F^e \mu_e^3 - \frac{m_e^2}{2} k_F^e \mu_e - \frac{m_e^4}{2} \ln \left(\frac{k_F^e + \mu_e}{m_e} \right) \right] + V_F^{(1)}(\sigma),
\end{aligned} \tag{24}$$

$$\begin{aligned}
p = & -\frac{1}{2} m_\sigma^2 \sigma^2 + \frac{1}{2} m_\omega^2 \omega_0^2 + \frac{1}{2} m_\rho^2 R_{0,0}^2 \\
& + \sum_{\alpha=p,n} \frac{1}{12\pi^2} \left[(k_F^\alpha)^3 \mu_\alpha^* - \frac{3}{2} m^{*2} k_F^\alpha \mu_\alpha^* + \frac{3}{2} m^{*4} \ln \left(\frac{k_F^\alpha + \mu_\alpha^*}{m^*} \right) \right] \\
& + \frac{1}{12\pi^2} \left[(k_F^e)^3 \mu_e - \frac{3}{2} m_e^2 k_F^e \mu_e + \frac{3}{2} m_e^4 \ln \left(\frac{k_F^e + \mu_e}{m_e} \right) \right] - V_F^{(1)}(\sigma).
\end{aligned} \tag{25}$$

By setting $k = 0$ in Eqs. (5) and (6), one obtains the energies of nucleons and anti-nucleons at zero momentum. The critical density ρ_C for nucleon–anti-nucleon pair creation is defined at $E_- = M_N$ for $k = 0$.

III. NEUTRON STAR MATTER AND STRUCTURE

The parameters of the model are fitted to the ground state properties of spherical nuclei [28]. The RHA0 set of parameters gives $g_\sigma^2(M_N/m_\sigma)^2 = 229.67$, $g_\omega^2(M_N/m_\omega)^2 = 146.31$, $g_\rho^2(M_N/m_\rho)^2 = 151.90$. It leads to the nuclear matter saturation density $\rho_0 = 0.1513\ fm^{-3}$ with a binding energy $E_{bind} = -17.39$ MeV and a bulk symmetry energy $a_{sym} = 40.4$ MeV.

Fig. 2 depicts the binding energy per nucleon as a function of baryon density for pure neutron matter, symmetric nuclear matter and neutron star matter. The corresponding relations of pressure and energy density are given in Fig. 3. In all these calculations the vacuum contributions have been taken into account. One can see that the equation of state becomes much stiffer in the case of pure neutron matter and neutron star matter. We note that the causal limit, $p = \epsilon$, is respected by the relativistic Hartree approach employed here. Fig. 4 displays the potentials and the nucleon effective mass as a function of baryon density. It can be found that the scalar potential approaches to saturation at high density while the vector potential increases rapidly with the increase of density. Due to the absence of hyperons, the neutral ρ-meson field exhibits a monotonically increasing behavior.

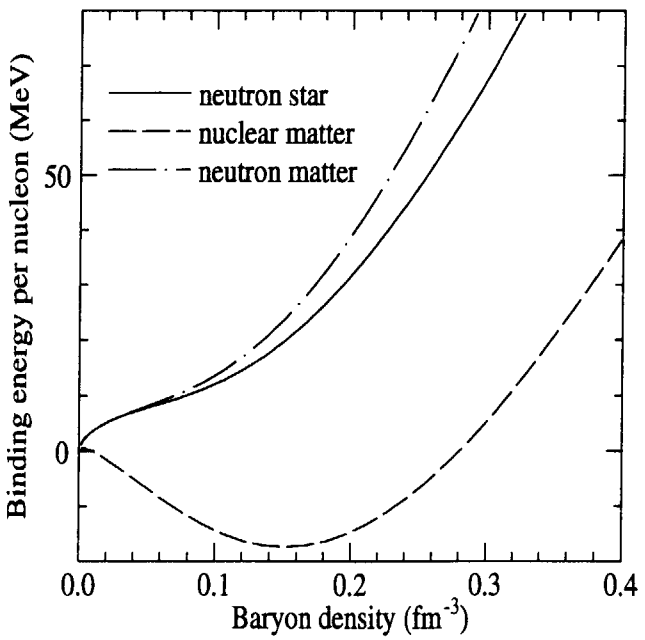

FIG. 2. The binding energy per nucleon as a function of baryon density.

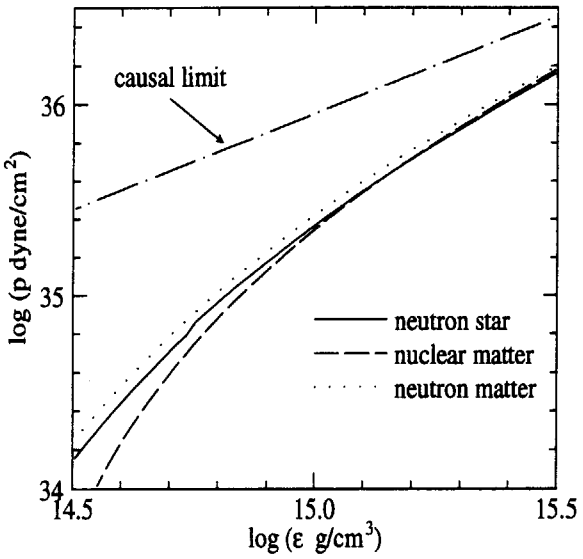

FIG. 3. Equation of state p .vs. ϵ of pure neutron matter, symmetric nuclear matter and neutron star matter.

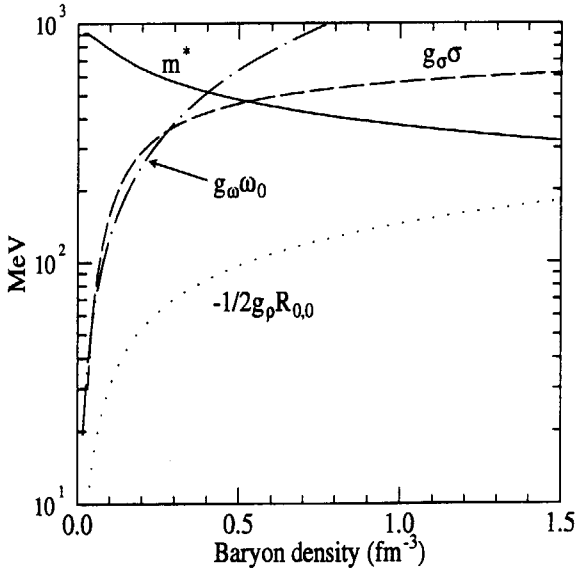

FIG. 4. The nucleon effective mass, scalar potential, vector potential and vector-isovector potential as a function of baryon density.

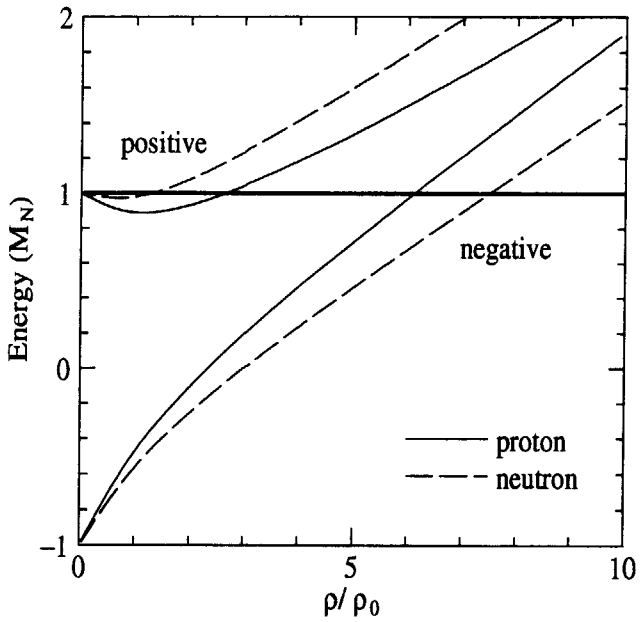

FIG. 5. The single-particle energies of the positive-energy nucleon and the negative-energy nucleon in neutron star matter.

In Fig. 5 we plot the single-particle energies of the positive-energy nucleon and the negative-energy nucleon at zero momentum as a function of density in neutron star matter. Since in neutron star matter ρ_0^n is larger than ρ_0^p, the neutral ρ-meson field $R_{0,0}$ is negative as can be seen from Eqs. (9) and (13). Thus, in the positive-energy sector, the energy of neutron is larger than that of proton while the situation becomes inverse in the negative-energy sector (please see Eqs. (5) and (6)). Consequently, the critical density of the $p\bar{p}$ pair creation $\rho_C^{p\bar{p}}$ is smaller than that of the $n\bar{n}$ pair creation $\rho_C^{n\bar{n}}$: $\rho_C^{p\bar{p}} = 6.1\ \rho_0$ and $\rho_C^{n\bar{n}} = 7.5\ \rho_0$. That means that the $p\bar{p}$ pair creation is energetically more favorable.

The structures and properties of neutron stars can be obtained by applying the equation of state to solve the Oppenheimer-Volkoff equation [30]. Fig. 6 shows the neutron star mass as a function of central energy density. Since the hyperon degrees of freedom are absent in the current model, the maximum mass of stars turns out to be $M_{max} = 2.44\ M_\odot$, with the corresponding radius $R = 12.75$ km and the central density $\rho_{cen} = 5.0\ \rho_0$.

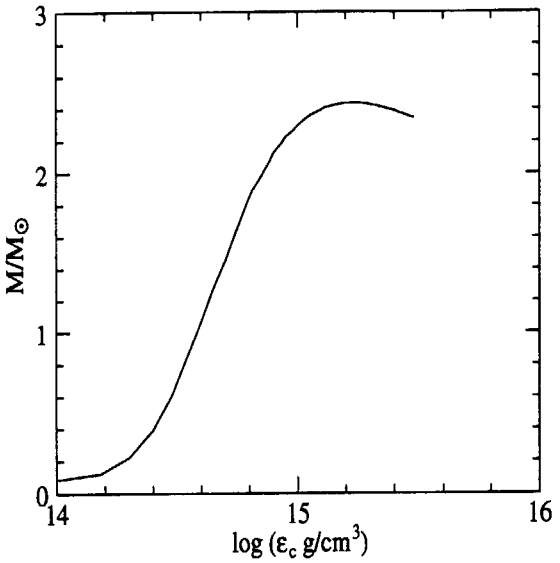

FIG. 6. Neutron star masses as a function of central energy density.

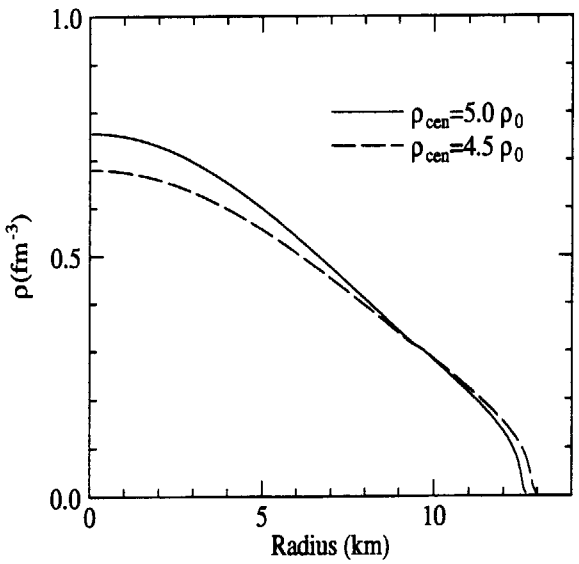

FIG. 7. Baryon density as a function of Schwarzschild radial coordinate.

The ρ_{cen} is smaller than both two critical densities $\rho_C^{p\bar{p}}$ and $\rho_C^{n\bar{n}}$. That means that the spontaneous $N\bar{N}$ pair creation does not happen at single neutron star within the model employed. In Fig. 7 we plot the density profiles of two neutron stars with the central densities $\rho_{cen} = 5.0\ \rho_0$ and $4.5\ \rho_0$, respectively. One can find that in the central core of neutron star the density decreases moderately with the increase of Schwarzschild radial coordinate.

IV. NEUTRON STAR COLLISIONS AND GAMMA-RAY BURSTS

We consider the following case of neutron star collision: Two identical neutron stars with $\rho_{cen} = 4.5\ \rho_0$ (with the current EOS, it is related to $M = 2.43\ M_\odot$ and $R = 13.0$ km) collide with each other. The impact parameter b stays between 0 and R, which determines the factor of density enhancement. We assume that a compact object of average density $7.2\ \rho_0$ is created in the reaction zone. The radius of the compact object is assumed to be $r = 1$ km (case A) or $r = 3$ km (case B) depending on the values of b. Since at single neutron star with $\rho_{cen} = 4.5\ \rho_0$ the density at $r = 1$ km is $4.46\ \rho_0$ and at $r = 3$ km is $4.18\ \rho_0$ (see, Fig. 7), in case A the density is enhanced during neutron star collision by a factor around 1.6 while in case B around 1.7. In both cases the $p\bar{p}$ pair creation will happen while the contributions of the $n\bar{n}$ pair creation is negligible (it contributes in at higher density but does not affect our discussions). We define a *Dirac momentum* k_D which describes the negative-energy nucleons occupying the eigenstates of the Dirac sea from the *toppest* level (the lowest-energy level) until the negative continuum (see, Fig. 1), i.e., $E_- = -M_N$ in Eq. (6). At the critical density of $p\bar{p}$ pair creation $\rho_C^{p\bar{p}} = 6.1\ \rho_0$, the potentials are: $g_\sigma\sigma = 556.8$ MeV, $g_\omega\omega_0 = 1183.0$ MeV and $1/2 g_\rho R_{0,0} = -137.5$ MeV. Inserting those values into Eq. (6), one obtains the *Dirac* momentum $k_D^C = 11.28\ fm^{-1}$. Similarly, at $\rho = 7.2\ \rho_0$, $g_\sigma\sigma = 578.9$ MeV, $g_\omega\omega_0 = 1393.5$ MeV and $1/2 g_\rho R_{0,0} = -150.8$ MeV, which gives $k_D = 12.45\ fm^{-1}$. We further define a momentum p_{max} at $E_- = M_N$, which turns out to be

$$p_{max} = \sqrt{\left(g_\omega\omega_0 - \frac{1}{2}g_\rho\tau_0 R_{0,0} + g_\sigma\sigma - 2M_N\right)\left(g_\omega\omega_0 - \frac{1}{2}g_\rho\tau_0 R_{0,0} - g_\sigma\sigma\right)}. \qquad (26)$$

Based on the semi-classical phase-space assumption we then estimate the number of the $p\bar{p}$ pairs whose energies are larger than the nucleon free mass at $\rho = 7.2\ \rho_0$ as

$$N_{pair} = \frac{4}{3}\pi r^3 \times \frac{p_{max}^3}{3\pi^2} = 2.147 r^3 \times 10^{54}. \tag{27}$$

Let us check whether most of the $p\bar{p}$ pairs can be emitted spontaneously. The rate of the $N\bar{N}$ pair production per unit surface area and unit time, $dN_{pair}/dSdt$, has been calculated in Ref. [27] for compressed matter. In the case of $\rho = 7\ \rho_0$ and tunnel distance $d = 1\ fm$, the rate turns out to be $2.68 \times 10^{-2}\ fm^{-3}$. For case B of $r = 3\ km$, the time needed to emit the available $p\bar{p}$ pairs is $t = 1.9 \times 10^{19}\ fm = 6.3 \times 10^{-5}\ s$, which is smaller than the typical dynamical scale of NS-NS collision $\tau \sim 10^{-3}\ s$. If one assumes that 80% of the produced anti-protons annihilate with protons in the surrounding medium and the released energy is 2 GeV at each event, the total exploded energy E_{tot} turns out to be 5.5×10^{51} erg and 1.5×10^{53} erg for case A and case B, respectively.

Some discussions are on time now. Neutron star collisions have repeatedly been suggested in the literature as possible sources of γ-ray bursts [31,32], powered either by $\nu\bar{\nu}$ annihilation or by highly relativistic shocks. In Ref. [22] Ruffert and Janka claimed that a γ-ray burst powered by neutrino emission from colliding neutron stars is ruled out. Here we propose a new scenario caused by the strong interactions in dense matter. A large number of anti-particles may be created from the vacuum when the density is higher than the critical density for spontaneous particle–anti-particle pair creation. Such high density can be reached during the NS-NS collisions, BH-NS mergers, or even NS-NS mergers when the merged binary neutron stars have large maximum densities. Some of produced anti-particles can be ejected from the reaction zone due to violent dynamics. They may be measured by detectors. Most of them will undertake dynamical procedure and annihilate with the corresponding particles at the ambient medium, and thus release a large amount of energy. As a first step we have discussed the $p\bar{p}$ pair creation in two neutron star collision since its critical density is lower than that of other baryons. Our calculations show that the exploded energy satisfies the requirement of the initial energy of the most energetic GRBs observed up to now. The variation of the released energies of different

GRBs can be attributed to the different impact parameters of colliding neutron stars. Those anti-protons, although produced spontaneously, annihilate during the dynamical procedure with a random probability to collide with protons. This leads to the observed burst duration. Furthermore, the anti-protons annihilate later might be accelerated by the photons produced by the nearby $p\bar{p}$ pair annihilation taking place earlier. This leads to the high-energy anti-protons and, consequently, the high-energy photons. Some of them may escape from the fireball before being distorted by the medium. Those escaped high-energy photons can constitute the observed high-energy tail of γ-ray bursts. We suggest to measure the anti-proton spectrum, especially the high-energy anti-protons which may not be produced via baryon-baryon scatterings during dynamics, from the identical source of a γ-ray burst, as a test of the proposed scenario.

V. SUMMARY AND OUTLOOK

We have proposed a new scenario of vacuum discharge due to strong interactions in dense matter as a possible source of γ-ray bursts. Based on the meson-exchange model we have estimated the exploded energy $E_{tot} \sim 10^{51} - 10^{53}$ erg, which fits well into the range of the initial energy of the most energetic γ-ray bursts. For a more quantitative study, one needs to introduce hyperon degrees of freedom [24] and even quark degree of freedom [33] if one assumes that the center of neutron star is in quark phase. A relativistic microscopic dynamical model like relativistic Quantum Molecular Dynamics is highly desirable to simulate NS-NS collisions, NS-NS/BH-NS mergers. Works on these aspects are presently underway.

ACKNOWLEDGEMENTS

The authors thank H. Takemoto, V. Kondratyev and A. Iwamoto for fruitful discussions. G. Mao acknowledges the STA foundation for financial support and the people of Research Group for Hadron Science at Japan Atomic Energy Research Institute for their hospitality.

References

[1] R.W. Klebesadel, I.B. Strong, R.A. Olson, Astrophs. J. Lett. **182**, L85 (1973).

[2] E. Costa et al., Nature **387**, 783 (1997).

[3] J. van Paradijs et al., Nature **386**, 686 (1997).

[4] D.A. Frail, S.R. Kulkarni, L. Nicastro, M. Feroci, and G.B. Taylor, Nature **389**, 261 (1997).

[5] M.R. Metzger et al., Nature **387**, 878 (1997).

[6] S.R. Kulkarni et al., Nature **393**, 35 (1998).

[7] S.G. Djorgovski et al., CGN notice **139**, 1998.

[8] S.R. Kulkarni et al., Nature **398**, 389 (1999).

[9] Tsvi Piran, Phys. Rep. **314**, 575 (1999).

[10] P. Kumar, astro-ph/9907096.

[11] K. Hurley et al., Nature **372**, 652 (1994).

[12] D. Eichler, M. Livio, T. Piran, and D.N. Schramm, Nature **340**, 126 (1989).

[13] M. Shibata, T. Nakamura, K. Oohara, Prog. Theor. Phys. **88**, 1079 (1992); Prog. Theor. Phys. **89**, 809 (1993);

[14] F.A. Rasio and S.L. Shapiro, Astrophys. J. **432**, 242 (1994).

[15] M. Ruffert, H.-Th. Janka, K. Takahashi, and G. Schäfer, Astron. Astrophys. **319**, 122 (1997).

[16] K.S. Cheng and Z.G. Dai, Phys. Rev. Lett. **77**, 1210 (1996).

[17] D. Fargion, astro-ph/9903433.

[18] R.N. Mohapatra, S. Nussinov, V.L. Teplitz, astro-ph/9909376.

[19] H.-Th. Janka and M. Ruffert, Astron. Astrophys. **307**, L33 (1996); M. Ruffert and H.-Th. Janka, Astron. Astrophys. **344**, 573 (1999).

[20] F.A. Rasio and S.L. Shapiro, Astrophys. J. **401**, 226 (1992).

[21] J.M. Centrella and S.L.W. McMillan, Astrophys. J. **416**, 719 (1993).

[22] M. Ruffert and H.-Th. Janka, Astron. Astrophys. **338**, 535 (1998).

[23] H.-Th. Janka, T. Eberl, M. Ruffert, and C.L. Fryer, astro-ph/9908290.

[24] N.K. Glendenning, Astrophs. J. **293**, 470 (1985); Nucl. Phys. **A493**, 521 (1989).

[25] B. D. Serot and J. D. Walecka, Adv. Nucl. Phys. **16**, 1 (1986).

[26] W. Greiner, Heavy Ion Physics **2**, 23 (1995).

[27] I.N. Mishustin, L.M. Satarov, J. Schaffner, H. Stöcker and W. Greiner, J. Phys. G: Nucl. Part. Phys. **19**, 1303 (1993).

[28] G. Mao, H. Stöcker, and W. Greiner, Int. J. Mod. Phys. **E8**, 389 (1999).

[29] S.A. Chin, Ann. Phys. **108**, 301 (1977).

[30] S.L. Shapiro and S.A. Teukolsky, *Black Holes, White Dwarfs and Neutron Stars* (Wiley, New York, 1983); N.K. Glendenning, *Compact Stars* (Springer, New York, 1997).

[31] J.I. Katz and L.M. Canel, Astrophys. J. **471**, 915 (1996).

[32] V.I. Dokuchaev, Yu.N. Eroshenko, Astronomy Letters **22**, 578 (1996).

[33] K. Schertler, S. Leupold, and J. Schaffner-Bielich, Phys. Rev. **C60**, 025801 (1999).

This is a blank page.

国際単位系 (SI) と換算表

表 1　SI基本単位および補助単位

量	名称	記号
長さ	メートル	m
質量	キログラム	kg
時間	秒	s
電流	アンペア	A
熱力学温度	ケルビン	K
物質量	モル	mol
光度	カンデラ	cd
平面角	ラジアン	rad
立体角	ステラジアン	sr

表 2　SIと併用される単位

名称	記号
分，時，日	min，h，d
度，分，秒	°，′，″
リットル	l，L
トン	t
電子ボルト	eV
原子質量単位	u

1 eV = 1.60218 × 10^{-19} J

1 u = 1.66054 × 10^{-27} kg

表 5　SI接頭語

倍数	接頭語	記号
10^{18}	エクサ	E
10^{15}	ペタ	P
10^{12}	テラ	T
10^{9}	ギガ	G
10^{6}	メガ	M
10^{3}	キロ	k
10^{2}	ヘクト	h
10^{1}	デカ	da
10^{-1}	デシ	d
10^{-2}	センチ	c
10^{-3}	ミリ	m
10^{-6}	マイクロ	μ
10^{-9}	ナノ	n
10^{-12}	ピコ	p
10^{-15}	フェムト	f
10^{-18}	アト	a

表 3　固有の名称をもつSI組立単位

量	名称	記号	他のSI単位による表現
周波数	ヘルツ	Hz	s^{-1}
力	ニュートン	N	m·kg/s^2
圧力，応力	パスカル	Pa	N/m^2
エネルギー，仕事，熱量	ジュール	J	N·m
工率，放射束	ワット	W	J/s
電気量，電荷	クーロン	C	A·s
電位，電圧，起電力	ボルト	V	W/A
静電容量	ファラド	F	C/V
電気抵抗	オーム	Ω	V/A
コンダクタンス	ジーメンス	S	A/V
磁束	ウェーバ	Wb	V·s
磁束密度	テスラ	T	Wb/m^2
インダクタンス	ヘンリー	H	Wb/A
セルシウス温度	セルシウス度	℃	
光束	ルーメン	lm	cd·sr
照度	ルクス	lx	lm/m^2
放射能	ベクレル	Bq	s^{-1}
吸収線量	グレイ	Gy	J/kg
線量当量	シーベルト	Sv	J/kg

表 4　SIと共に暫定的に維持される単位

名称	記号
オングストローム	Å
バーン	b
バール	bar
ガル	Gal
キュリー	Ci
レントゲン	R
ラド	rad
レム	rem

1 Å = 0.1 nm = 10^{-10} m

1 b = 100 fm^2 = 10^{-28} m^2

1 bar = 0.1 MPa = 10^5 Pa

1 Gal = 1 cm/s^2 = 10^{-2} m/s^2

1 Ci = 3.7 × 10^{10} Bq

1 R = 2.58 × 10^{-4} C/kg

1 rad = 1 cGy = 10^{-2} Gy

1 rem = 1 cSv = 10^{-2} Sv

（注）

1. 表1－5は「国際単位系」第5版，国際度量衡局 1985年刊行による。ただし，1 eVおよび1 uの値はCODATAの1986年推奨値によった。
2. 表4には海里，ノット，アール，ヘクタールも含まれているが日常の単位なのでここでは省略した。
3. barは，JISでは流体の圧力を表わす場合に限り表2のカテゴリーに分類されている。
4. EC閣僚理事会指令ではbar，barnおよび「血圧の単位」mmHgを表2のカテゴリーに入れている。

換算表

力	N(=10^5 dyn)	kgf	lbf
	1	0.101972	0.224809
	9.80665	1	2.20462
	4.44822	0.453592	1

粘度　1 Pa·s(N·s/m^2) = 10 P(ポアズ)(g/(cm·s))

動粘度　1 m^2/s = 10^4 St(ストークス)(cm^2/s)

圧力	MPa(=10 bar)	kgf/cm^2	atm	mmHg(Torr)	lbf/in^2(psi)
	1	10.1972	9.86923	7.50062 × 10^3	145.038
	0.0980665	1	0.967841	735.559	14.2233
	0.101325	1.03323	1	760	14.6959
	1.33322 × 10^{-4}	1.35951 × 10^{-3}	1.31579 × 10^{-3}	1	1.93368 × 10^{-2}
	6.89476 × 10^{-3}	7.03070 × 10^{-2}	6.80460 × 10^{-2}	51.7149	1

エネルギー・仕事・熱量	J(=10^7 erg)	kgf·m	kW·h	cal(計量法)	Btu	ft·lbf	eV
	1	0.101972	2.77778 × 10^{-7}	0.238889	9.47813 × 10^{-4}	0.737562	6.24150 × 10^{18}
	9.80665	1	2.72407 × 10^{-6}	2.34270	9.29487 × 10^{-3}	7.23301	6.12082 × 10^{19}
	3.6 × 10^6	3.67098 × 10^5	1	8.59999 × 10^5	3412.13	2.65522 × 10^6	2.24694 × 10^{25}
	4.18605	0.426858	1.16279 × 10^{-6}	1	3.96759 × 10^{-3}	3.08747	2.61272 × 10^{19}
	1055.06	107.586	2.93072 × 10^{-4}	252.042	1	778.172	6.58515 × 10^{21}
	1.35582	0.138255	3.76616 × 10^{-7}	0.323890	1.28506 × 10^{-3}	1	8.46233 × 10^{18}
	1.60218 × 10^{-19}	1.63377 × 10^{-20}	4.45050 × 10^{-26}	3.82743 × 10^{-20}	1.51857 × 10^{-22}	1.18171 × 10^{-19}	1

1 cal = 4.18605 J（計量法）

= 4.184 J　（熱化学）

= 4.1855 J　（15 °C）

= 4.1868 J（国際蒸気表）

仕事率　1 PS（仏馬力）

= 75 kgf·m/s

= 735.499 W

放射能	Bq	Ci
	1	2.70270 × 10^{-11}
	3.7 × 10^{10}	1

吸収線量	Gy	rad
	1	100
	0.01	1

照射線量	C/kg	R
	1	3876
	2.58 × 10^{-4}	1

線量当量	Sv	rem
	1	100
	0.01	1

（86年12月26日現在）

VACUUM DISCHARGE AS A POSSIBLE SOURCE OF GAMMA-RAY BURSTS